Ultra-Long Waves and Two-Dimensional Rossby Waves[1]

JOHN M. WALLACE AND HUANG-HSIUNG HSU

Department of Atmospheric Sciences, AK-40, University of Washington, Seattle, 98195

(Manuscript received 30 September 1982, in final form 29 April 1983)

ABSTRACT

The characteristics of planetary wave dispersion in the wintertime troposphere are investigated on the basis of 5 day mean 500 mb height data for 30 winters, making use of simple analysis techniques involving lag-correlation maps for individual gridpoints and for Fourier coefficients of zonal wavenumbers 1 and 2 on 50°N. It is shown that the time evolution of the planetary-waves is dominated by energy dispersion through longitudinally localized wavetrains with "great circle route" orientations, revealed most clearly by the lag-correlation maps for individual gridpoints. When the polarity of these localized patterns is such that large anomalies of like (opposing) sign appear in the Atlantic and Pacific sectors near 50°N, a strong zonal wavenumber 2 (1) pattern results. These wavenumber 1 and 2 patterns do not retain their identity from one 5 day period to the next as distinctly as the localized wavetrains do.

The conceptual model of Rossby-wave propagation along latitude circles still appears to be valid for the wintertime stratosphere, where the waves have the same two-dimensional scale as the polar vortex itself, and for external Rossby-modes such as those described by Madden (1978). It may also be valid at times in the Southern Hemisphere troposphere.

1. Introduction

The low-frequency variability of the ultra-long waves has been a recurrent theme in the literature on long range weather forecasting for more than four decades. Beginning with the influential papers of Rossby (1939, 1940) and continuing up to the recent review papers of Madden (1979) and Hayashi (1982), most of the work in this area has tended to emphasize Rossby-wave phase propagation along latitude circles. The wind, temperature and geopotential height fluctuations in these waves have tended (either explicitly or implicitly) to be represented by functions of the form

$$\Psi(y, z, t)e^{ik\lambda/2\pi},$$

where Ψ is a complex number representing both amplitude and phase, y is the latitude coordinate, z the vertical coordinate, t is time, k the zonal wavenumber (1 or 2 for the ultra-long waves) and λ is longitude. The need for documentation of the behavior of these ultra-long waves has given rise to an extensive observational literature based on a succession of increasingly sophisticated analysis techniques which can be classed under the general category of wavenumber–frequency analysis. Many of these works are summarized in Madden's and Hayashi's reviews. Among the significant achievements of this work are:

1) the documentation and dynamical interpretation of the sudden warming events in the lower stratosphere;

2) the identification of Kelvin-waves, mixed Rossby–gravity waves and other equatorially trapped wave modes in the lower stratosphere;

3) documentation of atmospheric tides and the discovery of rather regular, zonally propagating Rossby-waves in the upper stratosphere and mesosphere; and

4) the isolation of global, westward propagating external Rossby-wave modes with periods around 5 and 15 days.

The exploitation of the techniques of wavenumber–frequency analysis for the study of low-frequency planetary-wave variability has been hampered by the lack of strong temporal coherence between the respective sine and cosine coefficients. For example, according to Table 5a of Blackmon (1976), for the frequency band centered at 1 cycle per 15 days, the normalized quadrature spectrum between the respective sine and cosine coefficients of the dominant spherical harmonics associated with the planetary waves is only ~0.3. From this result it follows that only $(0.3)^2$ or ~10% of the variance of this mode is explicable in terms of a single zonally propagating wave. Some additional variance might be explained by taking into account the possibility that two ultra-long waves propagating in opposite directions might be contributing to the variance in this frequency band, but in any case the fraction of the variance that can be attributed to the passage of regular,

[1] Contribution No. 676, Department of Atmospheric Sciences, University of Washington.

zonally propagating, quasi-one dimensional waves is quite small.

The concept of Rossby-wave phase propagation and energy dispersion as inherently two-dimensional phenomena is deeply rooted in the geophysical fluid dynamics and oceanography literature [see, e.g., Longuet-Higgins (1964) and the reviews of Platzmann (1968) and Hoskins (1983)]. However, it is only recently that its relevance to atmospheric planetary waves has become widely recognized, largely as a result of the work of Hoskins *et al.* (1977). They considered Rossby-wave dispersion from localized sources on a sphere in a linearized barotropic model and showed that energy tends to disperse through geographically fixed wavetrains whose axes are oriented along broad arcs which resemble "great circle routes" rather than latitude circles. Hoskins and Karoly (1981) showed that a similar kind of wave dispersion occurs in a baroclinic model. These ideas have already been applied to the interpretation of numerical modeling results concerning the global response to tropical sea-surface temperature anomalies (Opsteegh and van den Dool, 1980; Webster, 1981, 1982; Shukla and Wallace, 1983).

The sophisticated, but rather specialized techniques of wavenumber-frequency analysis, which depend upon the manipulation of paired sine and cosine coefficients can, in principle, be extended to the description of two-dimensional Rossby-wave dispersion (Hayashi, 1981), but only at the expense of a considerable increase in complexity. An alternative, time-honored approach is to examine a judicious selection of one-point correlation maps. Recent examples of the use of this technique include documentations of Northern Hemisphere wintertime teleconnection patterns (Wallace and Gutzler, 1981) and planetary-wave phenomena associated with the Southern Oscillation (Horel and Wallace, 1981), both of which were limited to the consideration of simultaneous correlation patterns in monthly or seasonal mean data. Edmon (1980) and Lau (1981) have employed lag-correlations involving 5 day mean data (data generated by a general circulation model in Lau's study) to show some indication of the time evolution associated with the dominant teleconnection patterns. A more extensive discussion of this topic, together with a wider selection of lag-correlation charts based on filtered data, is presented in forthcoming articles by Blackmon *et al.* (1983a,b).

The one-dimensional and two-dimensional conceptual models of Rossby-wave dispersion represent alternative interpretations of the low-frequency variability of the planetary waves. The one-dimensional model is the more useful interpretation if waves are local in the wavenumber domain (in the sense that there are just a few zonal wavenumbers to contend with) and distributed in the longitude domain (i.e., simultaneously present along the entire length of latitude circles); whereas the two-dimensional model is more useful if they are distributed in the wavenumber domain and local in the longitude domain. There is ample evidence to support the view that both kinds of Rossby-wave dispersion exist within the earth's atmosphere, but it is not clear which one predominates.

A related question arises with respect to the one- and two-dimensional analysis approaches described above. The two approaches are so different from one another that it is not clear whether the resulting spectra and correlation maps should be viewed as complementary descriptions of the same wave dispersion phenomena or as descriptions of distinctly different phenomena which happen to occur in the same part of the atmosphere.

In this short note the above questions will be addressed by examining a set of relatively simple lag-correlation statistics derived from 30 winters of gridded geopotential-height data for the Northern Hemisphere.

2. Data and analysis procedures

The data set consists of gridded analyses of 500 mb height, prepared operationally, twice a day by the United States National Meteorological Center (NMC) and archived in the Data Library of the National Center for Atmospheric Research. For the period beginning 2 November 1948 and ending 31 March 1980, a gridded data set consisting of consecutive 5 day (pentad) means was prepared by H. J. Edmon. The pentads were defined in terms of calendar date (1–5 January being pentad number 1, 6–10 January being pentad number 2, etc.; 73 pentads per year, where grids for 29 February of leap years were omitted). In computing the pentad means, a small number of obviously erroneous grids were discarded and replaced by ones that were linearly interpolated in time from the neighboring grids.

The winter season was defined as the 30 pentads (150 days) extending from pentad number 62 through pentad number 18 of the following calendar year (2 November–31 March inclusive). Data for the 1959–60 and 1960–61 winters were discarded because of suspicious features near the (low-latitude) periphery of the grids, leaving a total of 30 winters (900 pentads) in the data set.

Before any further calculations were performed the annual cycle was removed by fitting a least squares parabola to each winter's data for each gridpoint and then subtracting it out. This operation has the effect of removing not only the climatological mean annual cycle but also the interannual variability of seasonal means plus a small part of the very low-frequency variability within seasons. It has virtually no effect upon the week-to-week variability, which tends to dominate in the lag-correlation statistics shown in the next section.

Harmonic analysis of the height anomalies along the 50°N latitude circle was used to compute the coefficients of the ultra-long waves. Here A_k and B_k refer to the cosine and sine coefficients of zonal wavenumber k, respectively, where the longitude angle is defined with respect to the Greenwich meridian and the units are in meters.

3. Results

If the low-frequency variability of the planetary waves is indeed local in the zonal wavenumber domain, then one should expect the paired cosine and sine coefficients of the individual zonal wavenumbers (k = 1 or 2) to show stronger lag-correlations with one another than with the coefficients of other zonal wavenumbers. If westward propagating waves with periods on the order of three weeks account for an appreciable fraction of the temporal variability of zonal wavenumber 1, as indicated by wavenumber-frequency analysis, then A_1 and B_1 should be positively correlated when B_1 leads A_1 by five days, and vice versa.

Table 1 shows lag-correlations between A_1 for 500 mb height and the other coefficients of the long waves, up to and including k = 4, for lags of −1, 0, and +1 pentad relative to A_1. In order to demonstrate the reproducibility of the results the data set is divided into odd and even years according to the year in which January falls, and lag-correlations are listed separately for the two subsets of the data.

In this case A_1 evidently shows some reproducible simultaneous correlations with the coefficients of some of the higher harmonics; particularly B_2 and B_4. Hence, zonal wavenumber 1 on 50°N tends to occur in combination with higher wavenumbers. The lag-correlations tend to be weaker than the simultaneous correlations, but many of them appear to be reproducible in the two subsets of the data. The fact that A_1 shows the strongest lag-correlation with itself rather than with B_1 indicates that zonal wavenumber 1 tends to oscillate as a standing wave with fixed nodes and antinodes or that fluctuations with periods longer than 20 days tend to predominate. The lag +1 correlation between A_1 and B_1 is in the proper sense to be consistent with westward phase propagation, but it is not much stronger than some of the lag correlations between A_1 and the coefficients of the higher wavenumbers. The lag −1 correlation between A_1 and B_1 is much weaker than the lag +1 correlation; if simple, westward propagating waves were dominant, one would expect the lag +1 and lag −1 correlations to be equal in strength but opposite in sign. Hence, there is reproducible structure in the correlations between A_1 and the other coefficients which suggests that coherent structures other than simple, westward propagating waves are present. Analogous results for A_2, displayed in Table 2, suggest similar conclusions with regard to zonal wavenumber 2.

TABLE 1. Temporal correlations between A_1 and the Fourier coefficients of zonal wavenumbers 1–4 for 5 day mean 500 mb height data on 50°N. The coefficients listed on the left are lagged relative to A_1 by the number of pentads listed at the top of the column. Results based on odd and even winters (according to the calendar year in which January falls) are listed separately.

	−1		0		+1	
Lag	Odd	Even	Odd	Even	Odd	Even
A_1	0.43	0.41	1.00	1.00	0.43	0.41
B_1	−0.06	−0.04	−0.25	−0.26	−0.32	−0.33
A_2	−0.19	−0.21	−0.23	−0.27	−0.22	−0.26
B_2	−0.08	−0.19	−0.18	−0.35	−0.12	−0.12
A_3	0.00	−0.09	0.20	0.06	0.19	0.11
B_3	−0.03	0.13	−0.03	0.03	−0.06	−0.21
A_4	−0.06	−0.11	−0.09	−0.06	−0.15	−0.08
B_4	−0.19	−0.35	−0.28	−0.36	−0.12	−0.11

TABLE 2. As in Table 1, but for A_2.

	−1		0		+1	
Lag	Odd	Even	Odd	Even	Odd	Even
A_1	−0.22	−0.26	−0.23	−0.27	−0.19	−0.21
B_1	0.00	0.14	0.08	0.17	0.12	0.06
A_2	0.40	0.33	1.00	1.00	0.40	0.33
B_2	0.23	0.26	0.04	0.06	−0.21	−0.16
A_3	−0.07	0.02	−0.04	−0.06	−0.09	−0.15
B_3	−0.06	0.03	−0.23	−0.06	−0.10	0.02
A_4	0.04	0.06	0.32	0.33	0.29	0.31
B_4	0.25	0.25	0.21	0.25	0.13	0.20

Figure 1 shows the pattern of simultaneous correlation between A_1 on the same 50°N latitude circle and 500 mb height at individual gridpoints throughout the hemisphere. Before looking at the pattern itself, it is perhaps worth reflecting on the interpretation of such a correlation map. If one were to attempt to specify 500 mb height Z at gridpoint J on the basis of a linear relationship with A_1 on 50°N, the correlation coefficient $r(Z_J, A_1)$ plotted on the map gives the specified normalized 500 mb height anomaly at J when A_1 exhibits a positive anomaly of one standard deviation. To state it in more qualitative terms, the correlation pattern in Fig. 1 shows the pattern of typical normalized 500 mb height anomalies when A_1 on 50°N is positive. The squared correlation $r^2(Z_J, A_1)$, which can be readily inferred from the map, gives the fraction of the temporal variance of 500 mb height anomalies at J that can be inferred on the basis of a knowledge of A_1 on 50°N.

The pattern in Fig. 1 is dominated by a strong zonal wavenumber 1 component along 50°N with a maximum near 20°W and a minimum near 170°W; the 150° separation between maximum and minimum being a reflection of higher harmonics in the correlation pattern. In the vicinity of these centers the cosine coefficient of zonal wavenumber 1 accounts

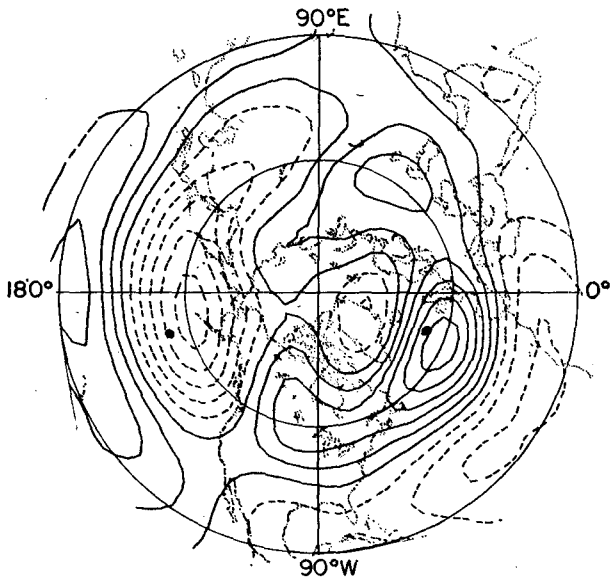

FIG. 1. Simultaneous correlation between A_1 (the cosine coefficient of zonal wavenumber 1 referred to the Greenwich meridian) on 50°N and individual gridpoint values of 500 mb height, based on 5 day mean data for 30 winters. Contour interval 0.1; negative contours ≤ 0.1 are dashed. The solid circles refer to gridpoints for which one-point lag-correlation maps are shown in Fig. 3.

for $\sim(0.55)^2$ or 30% of the temporal variance of the 500 mb height anomalies in the 5 day mean data. There is a well-defined node in the pattern near 33°N and a subtropical regime in which $k = 1$ appears with reversed phase. There is also evidence of a higher latitude node near 70°N. Such a meridional structure is consistent with previous results of Blackmon (1976), who showed that for the low frequency fluctuations in spherical harmonics associated with zonal wavenumber 1, most of the variance is distributed among the meridional modes with 1, 2, and 3 zero crossings between equator and pole. Madden (1978) also found evidence of a midlatitude node in the meridional structure of low-frequency fluctuations in zonal wavenumber 1.

The strong geometrical symmetry of the correlation pattern is evidence that this analysis technique has been reasonably successful in isolating zonal wavenumber 1, as it was intended to do. Yet there are some asymmetries in the pattern that bear mentioning. The strong correlations tend to be more concentrated over the oceanic sectors of the hemisphere than one would expect in the case of a pure zonal wavenumber 1 pattern. Part of the dominance of the oceanic sectors can be ascribed to the fact that 500 mb height exhibits larger low-frequency variability over the northern oceans than over the land-masses (e.g., see Blackmon, 1976, Fig. 4a). However, the resemblance of the pattern in Fig. 1 over the oceanic sectors to the "East Atlantic" and "Pacific/North American" teleconnection patterns described by Wallace and Gutzler (1981) and others before them is suggestive of a possible link to two-dimensional

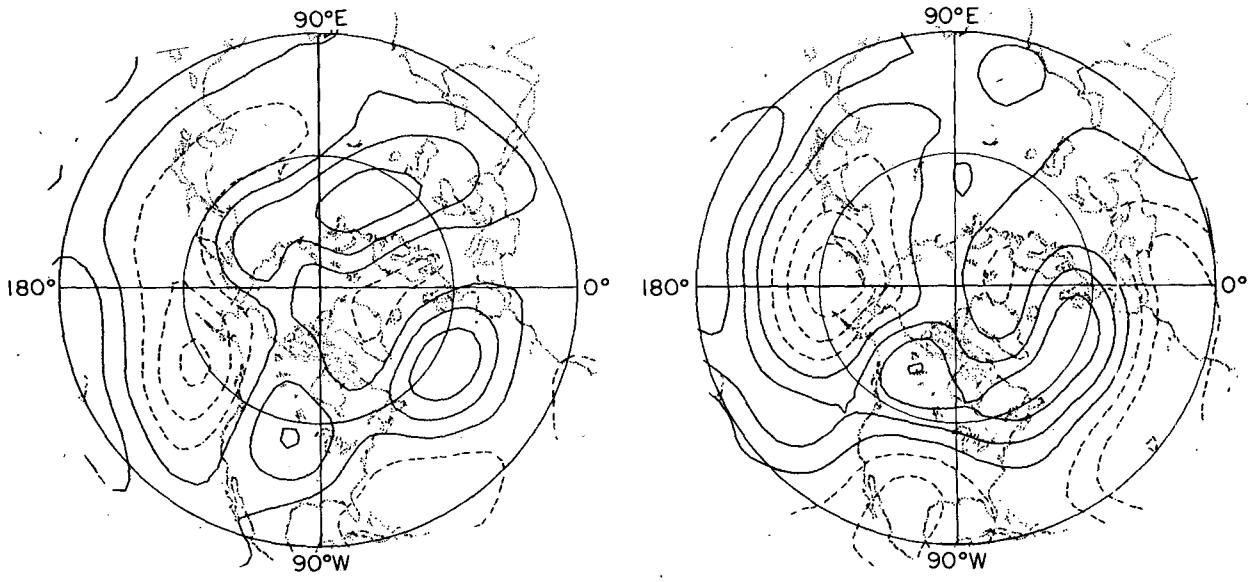

FIG. 2. Lag-correlation between A_1 on 50°N and individual gridpoint values of 500 mb height (a) for the pentad five days earlier, and (b) for the pentad five days later. Contour interval 0.1; negative contours ≤ 0.1 are dashed.

Rossby-wave dispersion. The use of lag-correlation charts will enable us to explore this possibility further.

Figure 2 shows the lag correlation patterns for A_1 on the 50°N latitude circle and 500 mb height throughout the hemisphere: a) one pentad earlier, and b) one pentad later. Before examining these patterns in detail it may be worth considering how to interpret them. If one-dimensional Rossby-wave phase propagation is predominant, then the zonal wavenumber 1 pattern in Fig. 1 should retain its identity in the lag-correlation maps, with a shift in longitudinal phase consistent with its period and direction of propagation. For example, if it propagates westward with a period on the order of 20 days, its phase in Fig. 2a should be ~90° further east than in Fig. 1 and in Fig. 2b it should be 90° further west than in Fig. 1. On the other hand, if two-dimensional Rossby-wave dispersion is dominant, we might expect the major features in Figs. 2a, 1, and 2b to occur in approximately the same geographical locations but with changes in relative strength consistent with the notion of energy dispersion along great circle arcs (i.e., upstream centers of action accentuated in Fig. 2a and downstream centers accentuated in Fig. 2b).

Some of the features in Fig. 2 do, in fact, show evidence of a slight westward phase propagation; for example, the north–south dipole pattern over the Pacific sector shifts westward by ~30° of longitude over the 10 day interval from Fig. 2a to Fig. 2b. However, there are other distinctions between the figures which are, perhaps, more important. The patterns in Fig. 2 represent a superposition of several zonal wavenumbers: zonal wavenumber 1 is present but it is not nearly as dominant as in Fig. 1. Figure 2a contains elements of the Pacific/North American and Eurasian patterns described by Wallace and Gutzler (1981), and Fig. 2b contains elements of the Pacific/North American and "Eastern Atlantic" patterns.

The relation of the patterns in Fig. 2 to the Pacific/North American and Eastern Atlantic patterns is demonstrated more convincingly by comparing them to the one-point lag-correlation maps for base gridpoints located near the primary centers of action of those patterns, shown in Fig. 3. Note that the maps in Fig. 3 are split in half, with the pattern for the Pacific gridpoint on the lower left and that for the Atlantic gridpoint on the upper right segment of each panel.

The lower-left segments of Fig. 3 give some indication of the pattern of energy dispersion associated with the Pacific/North American pattern. The locations of the centers of action of the pattern change relatively little from Fig. 3a to 3b, but there is an intensification of the down-stream centers of action over North America as energy disperses eastward from the Pacific center of action along a broad "great circle" arc. These subtle changes are mirrored in the respective lower-left portions of Fig. 2. There is also a strong similarity between the patterns in the Atlantic/European sectors in Figs. 2 and 3, which are dom-

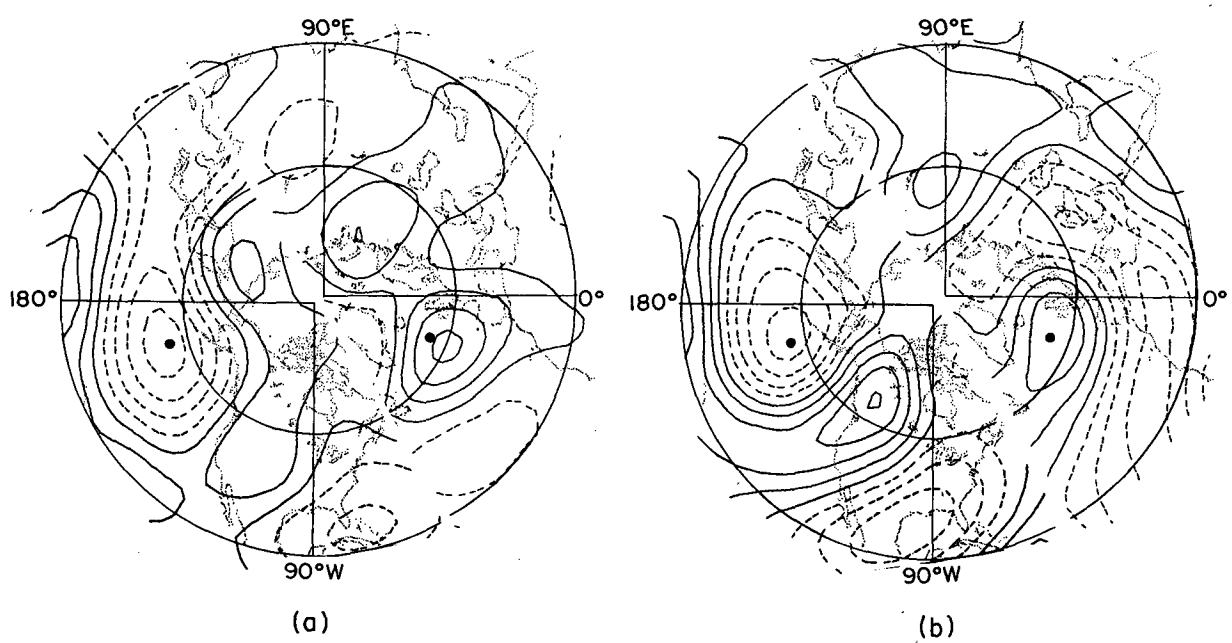

FIG. 3. Lag-correlations between 500 mb height at (45°N, 165°W) (left side) and (55°N, 20°W) (right side) and 500 mb height at individual gridpoints throughout the hemisphere (a) for the pentad five days earlier, and (b) for the pentad five days later. Contour interval 0.1; negative contours ≤ 0.1 are dashed. The polarity of the pattern for (45°N, 165°W) has been reversed. The positions of the two "base gridpoints" relative to the zonal wavenumber 1 pattern are indicated in Fig. 1.

inated by the Eastern Atlantic pattern. Hence, the time evolution of the zonal wavenumber 1 pattern in Fig. 1 is strongly influenced by Rossby-wave dispersion along separate "great circle" arcs in the Atlantic and Pacific sectors.

The above analysis was repeated for various linear combinations of A_1 and B_1, representing different phases of zonal wavenumber 1 relative to the Greenwich meridian. Results for a reference longitude of 45°E (not shown) are very similar to those described above, with energy dispersion through the geographically fixed Pacific/North American and Eastern Atlantic patterns. For a reference longitude of 90°E, the simultaneous correlation pattern shown in Fig. 4b is dominated by a north–south dipole pattern centered at 60°W which strongly resembles the Western Atlantic teleconnection pattern described by Wallace and Gutzler (1981). The eastward displacement of the strongest positive correlations relative to the reference longitude (90°E, W) is consistent with the negative simultaneous correlation between A_1 and B_1 in Table 1. The lag-correlation pattern for the previous pentad, shown in Fig. 4a, is characterized by a wavetrain with a great circle orientation extending across the eastern Pacific into central North America, while the pattern for the following pentad shows evidence of waves dispersing

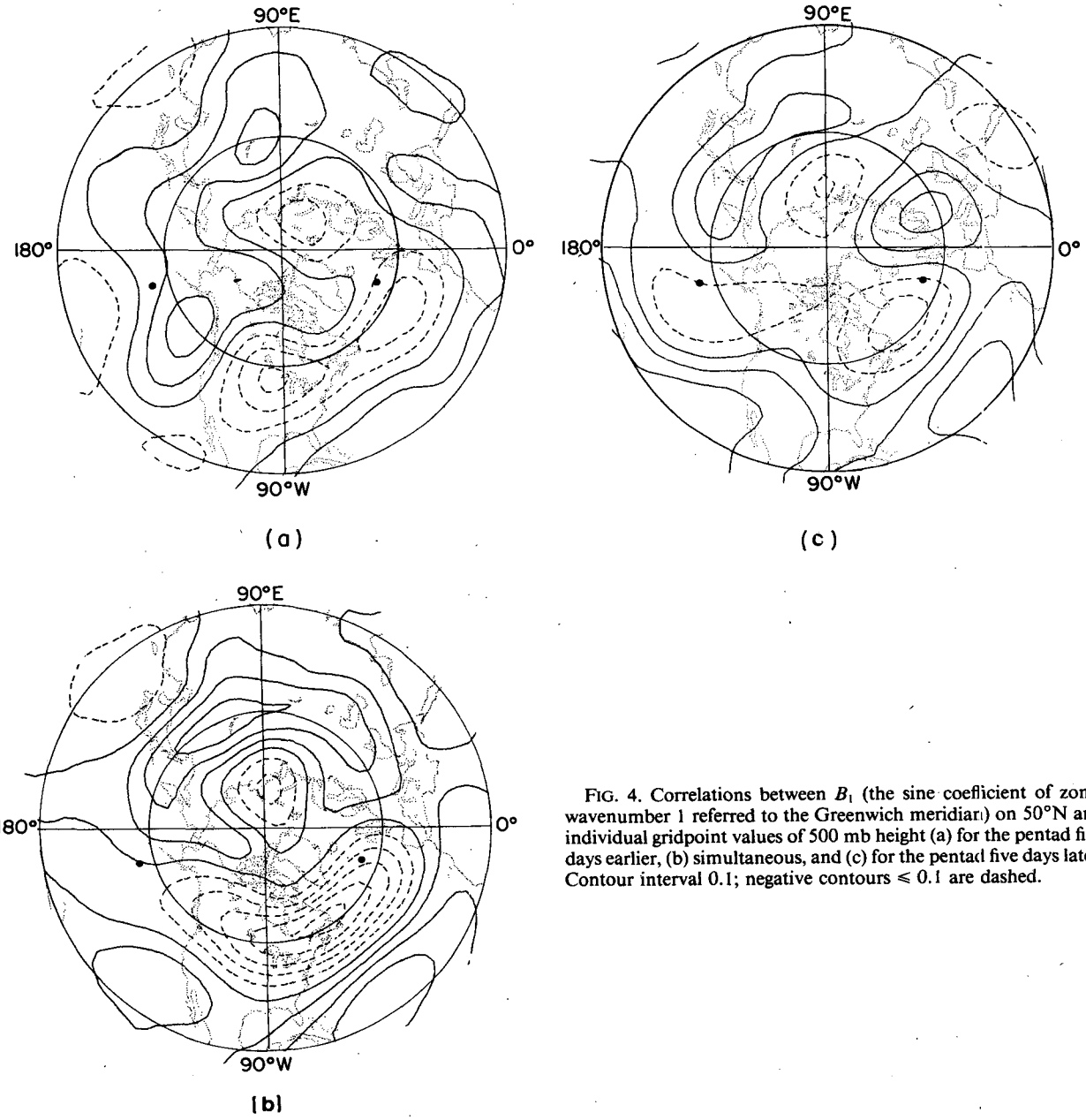

FIG. 4. Correlations between B_1 (the sine coefficient of zonal wavenumber 1 referred to the Greenwich meridian) on 50°N and individual gridpoint values of 500 mb height (a) for the pentad five days earlier, (b) simultaneous, and (c) for the pentad five days later. Contour interval 0.1; negative contours ≤ 0.1 are dashed.

along an arc extending across the Atlantic into Europe. Results for a reference longitude of 135°E (not shown) resemble those for 0°, but all the signs are reversed; the Pacific/North American and Eastern Atlantic patterns are evident in the simultaneous correlations and in the lag-correlations for the following pentad.

Analogous results for the cosine coefficient of zonal wavenumber 2 are presented in Figs. 5 and 6. The simultaneous correlation pattern (Fig. 5) shows a node in the meridional structure near 35°N, but there is no evidence of a second, high latitude node as in the results for zonal wavenumber 1 (Fig. 1). The pattern shows a high degree of geometrical symmetry, but there is more than a hint of the same Pacific/North American teleconnection pattern that appeared in connection with zonal wavenumber 1. The same teleconnection pattern is dominant in the lag correlations. Note, in particular, the strong resemblance to the lag-correlation patterns for the Pacific gridpoint (Figs. 3b and 6). Patterns for other reference longitudes (not shown) are also characterized by two-dimensional Rossby-wave dispersion.

The analysis was repeated for zonal wavenumbers 1 and 2 on the 45° and 55° latitude circles, and the results were found to be generally similar to those described above apart from minor differences in the positions of the nodes in the meridional structure.

4. Discussion

On the basis of the results presented in the previous section it would be tempting to conclude that at tropospheric levels zonal wavenumbers 1 and 2 are nothing more than mathematical abstractions whose time variability is determined by essentially random superpositions of two-dimensional Rossby-wavetrains propagating through various sectors of the hemisphere. However, there are reasons for believing that the more traditional one-dimensional model of Rossby-wave dispersion may be a useful description of: 1) planetary waves in the winter stratosphere, 2) certain external Rossby-wave modes, and 3) planetary waves in the Southern Hemisphere troposphere at certain times during winter.

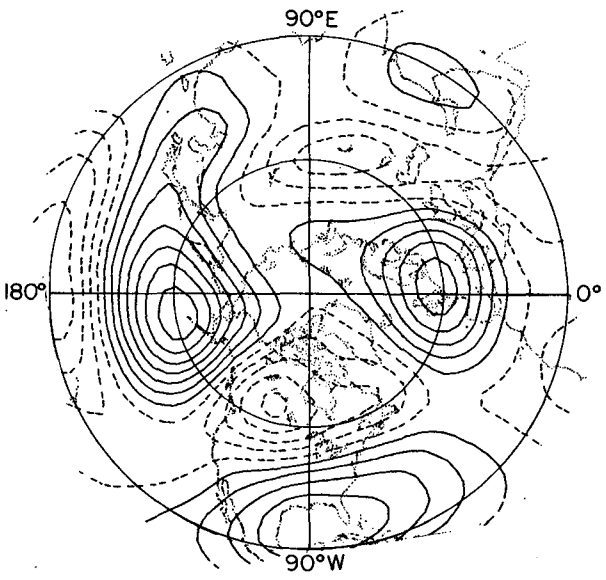

FIG. 5. Simultaneous correlation between A_2 on 50°N and individual gridpoint values of 500 mb height. Contour interval 0.1, negative contours ≤ 0.1 are dashed.

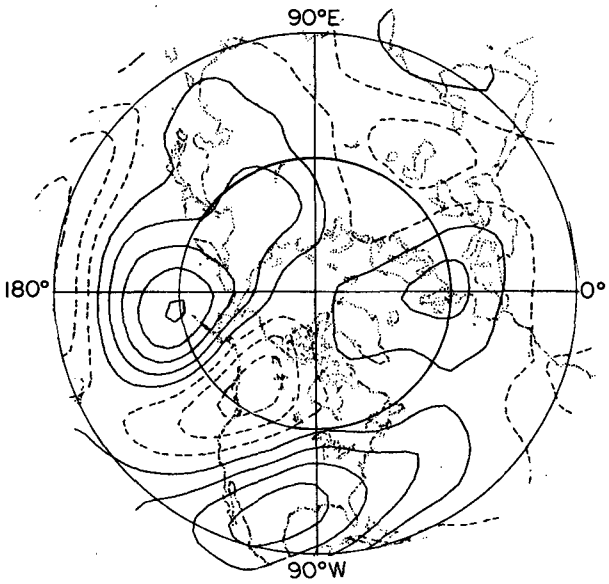

FIG. 6. Lag-correlation between A_2 on 50°N and individual gridpoint values of 500 mb height for the pentad five days later. Contour interval 0.1; negative contours ≤ 0.1 are dashed.

a. Contrasts between stratospheric and tropospheric planetary waves

At stratospheric levels individual zonal wavenumbers exhibit much stronger week-to-week time continuity than in the troposphere during wintertime, as evidenced by the distinctive wavenumber 1 and 2 warming events in both observed data and in numerical simulations. Furthermore, the distinctive two-dimensional wave dispersion patterns observed at the 500 mb level apparently do not extend into the stratosphere: individual synoptic maps for levels above 100 mb show no evidence of such features, and the senior author has examined one-point correlation maps for stratospheric levels and found them to be dominated by patterns of a much larger scale than those displayed in the previous section.

The ideas put forth by Charney and Drazin (1961) and generalized to three dimensions by B. J. Hoskins (personal communication, 1982) provide a theoretical explanation for this rather striking difference in the horizontal structure of the planetary waves between stratosphere and troposphere. Because the po-

lar-night vortex in the wintertime stratosphere is somewhat more intense and occurs at higher latitudes than the tropospheric jetstream, its degree of superrotation ω (relative to the earth's rotation rate Ω) is considerably larger. For typical wintertime conditions, $\omega/\Omega \sim 0.15$ at the level of the polar-night jet, whereas at the tropospheric jetstream level it is on the order of 0.05 at 50°N. The dispersion relation for stationary Rossby waves[2]

$$n(n+1) = \frac{2(\omega + \Omega)}{\omega},$$

where n is two dimensional wavenumber, implies the dominance of different spatial structures in the stratospheric and tropospheric planetary-waves. For the observed stratospheric superrotation, it is readily verified that $n \sim 3$–4, which is comparable to the scale of the polar-night vortex itself: hence the stratospheric planetary-waves cannot be local in the longitude domain. Furthermore, for meridional scales compatible with that of the polar night jet, the only possible zonal wavenumbers are 1 and 2. Such a high degree of localness in the wavenumber domain imposes strong geometrical constraints upon the kinds of wave patterns that can exist within the wintertime stratosphere. In contrast, the observed tropospheric superrotation is compatible with $n \sim 6$, which is substantially smaller than the scale of the tropospheric vortex so that the planetary waves assume the form of longitudinally local patterns consisting of combinations of zonal wavenumbers 1–4.

b. *External modes*

The westward-propagating ultra-long waves which have been detected in the wavenumber–frequency spectra of the 500 mb height field appear to be associated with coherent fluctuations whose amplitude increases with height throughout the troposphere and stratosphere (Madden, 1978; Pratt and Wallace, 1976; Mechoso and Hartmann, 1982). It seems unlikely that two-dimensional wave dispersion, which is largely confined to tropospheric levels, could account for the observed structure, which resembles that of an external Rossby mode (Madden). However it is plausible that it could be a major source of excitation for external modes.

c. *Southern Hemisphere wintertime planetary waves*

On some occasions the Southern Hemisphere wintertime planetary waves display a remarkable regularity which is suggestive of one-dimensional Rossby-wave dispersion. Figure 7 shows an example in which a strong zonal wavenumber 3 pattern persisted for about a month during midwinter with little change in phase. The phase-locked wavenumber 6 pattern at lower latitudes reinforces the impression of geometrical symmetry. Hamilton (1982) and Salby (1982) have shown evidence of a regular, zonally propagating zonal wavenumber 5 structure in the Southern Hemisphere troposphere.

FIG. 7. Time-averaged 500 mb height field for the Southern Hemisphere, based on ECMWF operational analyses for 1200 GMT for the period 6 July–4 August 1981. Contour interval 60 m.

Comparison of Northern and Southern Hemisphere wintertime climatological statistics of zonal wind (Oort and Rasmusson, 1971; van Loon, 1972; White, 1982) suggest that poleward of 45° the degree of superrotation is at least 50% larger in the Southern Hemisphere than the value quoted above for the Northern Hemisphere. The horizonal scale of the corresponding stationary waves should be closer to (two-dimensional wavenumber) $n = 5$, which is intermediate between the tropospheric and stratospheric ranges described above. Hence it is not inconceivable that the waves of this scale might at times assume a one-dimensional character, particularly if there were strong forcing in a particular zonal wavenumber.

The apparent dominance of two-dimensional wave dispersion in the Northern Hemisphere wintertime troposphere casts doubt upon spectral interpretations of low-frequency phenomena such as blocking and fluctuations in the intensity of the westerlies.

Acknowledgments. The discussion section developed out of discussions with Brian J. Hoskins at the

[2] Strictly speaking, the dispersion relation applies only to stationary Rossby-waves, but we use it here to make some qualitative inferences about the structure of low-frequency transient variability as well, since it should be applicable to disturbances with small-phase speeds.

University of Reading, where the senior author spent part of a recent sabbatical. This work was partially supported by the National Science Foundation, Climate Dynamics Research Section, under Grant 81-06099, and by a grant from the U.K. National Environmental Research Council.

REFERENCES

Blackmon, M. L., 1976: A climatological spectral study of the 500 mb geopotential height of the Northern Hemisphere. *J. Atmos. Sci.*, **33,** 1607–1623.

——, Y.-H. Lee and J. M. Wallace, 1983a: Horizontal structure of 500 mb height fluctuations with long, intermediate, and short time scales. *J. Atmos. Sci.* (submitted to).

——, ——, —— and H.-H. Hsu, 1983b: Time evolution of 500 mb height fluctuations with short, medium and long time scales. *J. Atmos. Sci.* (submitted to).

Charney, J. G., and P. G. Drazin, 1961: Propagation of planetary scale disturbances from the lower into the upper atmosphere. *J. Geophys. Res.*, **66,** 83–110.

Edmon, H. J., Jr., 1980: Time evolution of teleconnection patterns. *Proc. Fifth Annual Climate Diagnostics Workshop.* Seattle. NOAA, U.S. Dept. of Commerce, 85–92. [NTIS PB81-222200.]

Hamilton, K., 1983: Aspects of wave behavior observed in the mid and upper troposphere of the Southern Hemisphere. *Atmos. Ocean* (in press).

Hayashi, Y., 1981: Vertical-zonal propagation of a stationary planetary-wave packet. *J. Atmos. Sci.*, **38,** 1197–1205.

——, 1982: Space-time spectral analysis and its applications to atmospheric waves. *J. Meteor. Soc. Japan* (Centennial Issue), **60,** 156–171.

Horel, J. D., and J. M. Wallace, 1981: Planetary scale atmospheric phenomena associated with the Southern Oscillation. *Mon. Wea. Rev.*, **109,** 813–929.

Hoskins, B. J., 1983: Dynamical processes in the atmosphere and the use of models. *Quart. J. Roy. Meteor. Soc.*, **109,** 1–21.

——, and D. Karoly, 1981: The steady linear response of a spherical atmosphere to thermal and orographic forcing. *J. Atmos. Sci.*, **38,** 1179–1196.

——, A. J. Simmons and D. G. Andrews, 1977: Energy dispersion in a barotropic atmosphere. *Quart. J. Roy. Meteor. Soc.*, **103,** 553–567.

Lau, N.-C., 1981: A diagnostic study of recurrent meteorological anomalies appearing in a 15-year simulation with a GFDL general circulation model. *Mon. Wea. Rev.*, **109,** 2287–2311.

Longuet-Higgins, M. S., 1964: Planetary waves on a rotating sphere, I. *Proc. Roy. Soc. London,* **279,** 446–473.

Madden, R. A., 1978: Further evidence of traveling planetary waves. *J. Atmos. Sci.*, **35,** 1605–1618.

——, 1979: Observations of large-scale traveling Rossby waves. *Rev. Geophys. Space Phys.*, **17,** 1935–1949.

Mechoso, C. R., and D. L. Hartmann, 1982: An observational study of traveling planetary waves in the Southern Hemisphere. *J. Atmos. Sci.*, **39,** 1921–1935.

Oort, A. H., and E. M. Rasmusson, 1971: *Atmospheric Circulation Statistics.* NOAA Prof. Pap. No. 5, 323 pp. [NTIS COM-72-50295].

Opsteegh, J. D., and H. M. van den Dool, 1980: Seasonal differences in the stationary response of a linearized primitive equation model: prospects for long range forecasting? *J. Atmos. Sci.*, **38,** 554–571.

Platzman, G. W., 1968: The Rossby wave. *Quart. J. Roy. Meteor. Soc.*, **94,** 225–248.

Pratt, R. W., and J. M. Wallace, 1976: Zonal propagation characteristics of large-scale fluctuations in the mid-latitude troposphere. *J. Atmos. Sci.*, **33,** 1184–1194.

Rossby, C.-G., 1939: Relations between variations in the intensity of the zonal circulation and the displacements of the semi-permanent centers of action. *J. Mar. Res.*, **2,** 38–55.

——, 1940: Planetary flow patterns in the atmosphere. *Quart. J. Roy. Meteor. Soc.*, **66** (Suppl.), 68–87.

Salby, M. L., 1982: A ubiquitous wave 5 anomaly in the Southern Hemisphere during FGGE. *Mon. Wea. Rev.*, **110,** 1712–1720.

Shukla, J., and J. M. Wallace, 1983: Numerical simulation of the atmospheric response to equatorial Pacific sea-surface temperature anomalies. *J. Atmos. Sci.*, **40,** 1613–1630.

van Loon, H., J. J. Taljaard, T. Sasamori, J. London, D. V. Hoyt, K. Labitzke and C. W. Newton, 1972: *Meteorology of the Southern Hemisphere. Meteor. Monogr.* No. 35, Amer. Meteor. Soc., 263 pp.

Wallace, J. M., and D. S. Gutzler, 1981: Teleconnections in the geopotential height field during the Northern Hemisphere winter. *Mon. Wea. Rev.*, **109,** 785–812.

Webster, P. J., 1981: Mechanisms determining the atmospheric response to sea surface temperature anomalies. *J. Atmos. Sci.*, **38,** 554–571.

——, 1982: Seasonality in the local and remote atmospheric response to sea surface temperature anomalies. *J. Atmos. Sci.*, **39,** 41–52.

White, G. H., 1982: The global circulation of the atmosphere December 1980–November 1981 based upon ECMWF analyses. Published as a Tech. Note, Dept. Meteor., University of Reading, Berks., U.K.